# Multimodality Imaging Population Analysis using Manifold Learning

Jean-Baptiste Fiot, Laurent D. Cohen, Pierrick Bourgeat, Parnesh Raniga, Oscar Acosta, Victor Villemagne, Olivier Salvado, Jurgen Fripp

# Multimodality Imaging Population Analysis using Manifold Learning

Jean-Baptiste Fiot [1,2] Laurent D. Cohen [1] Pierrick Bourgeat [2] Parnesh Raniga [2]
Oscar Acosta[2,3,4] Victor Villemagne [5,6] Olivier Salvado [2] Jurgen Fripp [2]
[1] *CEREMADE, UMR 7534 CNRS Université Paris Dauphine, France*
[2] *CSIRO Preventative Health National Research Flagship ICTC,The Australian e-Health Research Centre - BioMedIA, Royal Brisbane and Women's Hospital, Herston, QLD, Australia*
[3] *INSERM, U 642, Rennes, F-35000, France*
[4] *Université de Rennes 1, LTSI, F-35000, France*
[5] *Department of Nuclear Medicine and Centre for PET, and Department of Medicine, University of Melbourne, Austin Hospital, Melbourne, VIC, Australia*
[6] *The Mental Health Research Institute, University of Melbourne, Parkville, VIC, Australia*

Characterizing the variations in anatomy and tissue properties in large populations is a challenging problem in medical imaging. Various statistical analysis, dimension reduction and clustering techniques have been developed to reach this goal. These techniques can provide insight into the effects of demographic and genetic factors on disease progression. They can also be used to improve the accuracy and remove biases in various image segmentation and registration algorithms. In this paper we explore the potential of some non linear dimensionality reduction (NLDR) techniques to establish simple imaging indicators of ageing and Alzheimers Disease (AD) on a large population of multimodality brain images (Magnetic Resonance Imaging (MRI) and PiB Positron Emission Tomography (PET)) composed of 218 patients including healthy control, mild cognitive impairment and AD. Using T1-weighted MR images, we found using laplacian eigenmaps that the main variation across this population was the size of the ventricles. For the grey matter signal in PiB PET images, we built manifolds that showed transition from low to high PiB retention. The combination of the two modalities generated a manifold with different areas that corresponded to different ventricle sizes and beta-amyloid loads.

**Keywords:** Population Analysis, Non Linear Dimensionality Reduction, Manifold Learning, Brain Imaging

## 1 INTRODUCTION

Analysing trends and modes in a population, as well as computing meaningful regressions, are challenges in the field of medical imaging. A considerable amount of work has been done to simplify the use of medical images for clinicians, and summarising the information in just few imaging biomarkers, that would for example quantify and easily allow the interpretation of disease evolution. This is of great interest not only for clinical diagnosis, but also to study clinical studies and stratify cohorts during clinical trials.

Large medical databases challenge manual analysis of a population. Unbiased atlases can be used to describe a population (Lorenzen et al. 2005). (Blezek and Miller 2007) introduced the atlas stratification technique, discovering modes of variation in a population using a mean shift algorithm. (Sabuncu et al. 2009) introduced iCluster, a clustering algorithm computing multiple templates that represent different modes in the population. (Davis et al. 2007) demonstrated the use of manifold kernel regression to regress the images with regard to a known parameter, such as age. (Wolz et al. 2009) introduced the Learning Embeddings for Atlas Propagation technique, and showed that the use of manifold learning can improve the segmentation results compared to the simple use of image similarity in multi-atlas segmentation techniques. (Gerber et al. 2010) developed a generative model to describe the population of brain images, under the assumption that the whole population derive from a small number of brains. These techniques usually rely on computations of diffeomorphisms or transformations to compute distances

between images. Alternatively it is also possible to use dimensionality reduction techniques directly on the image pixels intensities (Wolz et al. 2009), as we propose in this paper. Most dimensionality reduction techniques rely either on information theory or geometry. Information-based assumptions can be related to the maximum of variance (Principal Component Analysis (PCA), kernel Principal Component Analysis (kPCA)), entropy measure, etc. Geometric assumptions are either global (Multi Dimension Scaling (MDS), ISOmetric MAPping (ISOMAP)), or local (Local Linear Embeddings (LLE), Laplacian Eigenmaps (LEM), Hessian Eigenmaps (HEM), Diffusion Maps (DM), Local Tangent Space Alignment (LTSA)). References to these algorithms can be found in (van der Maaten et al. 2007).

In this publication, we examine the use of NLDR techniques to analyse multi-modality brain images. AD is associated with the deposition in the brain of amyloid plaques, which can be imaged with PET using the Pittsburgh compound B markers (PiB), and with brain atrophy, which can be imaged with MRI T1 weighted (T1-w) images. We are investigating the use of manifold learning techniques for studying PET-PiB and T1-w.

## 2 MATERIAL AND METHODS

### 2.1 Data

The dataset is composed of 218 patients from the AIBL study (Ellis et al. 2009). T1-w (image matrix 60x240x256, image spacing of 1.2x1x1 mm in the sagittal, coronal and axial directions, TR=2300ms, TR=2.98ms, TI=900ms, flip angle=9°) and PiB (reconstructed image matrix 28x128x90, 2x2x2mm spacing) scans were acquired.

### 2.2 Proposed Algorithm

The proposed algorithm, summarised in Fig. 1, consists of the following steps:

Pre-processing: PiB and MR images were affinely co-registered. All PiB Images were Standardised Uptake Value Ratio normalised to the mean uptake in the cerebellum crus region (Raniga et al. 2008). T1-w images were bias-field corrected in the mask creation process. T1-w images were then spatially normalised using an elderly brain atlas using affine and then non-rigid transformations. These transformations were then propagated to the PiB images. Noise was reduced in T1-w images using anisotropic diffusion, and in PiB images using a 2mm Gaussian convolution.

Mask creation: using a subset of 98 MR images, an average elderly brain atlas and its associated probabilistic tissue priors (grey matter (GM), white matter (WM) and cerebro-spinal fluid (CSF)) were created from the segmentations obtained using (Acosta et al. 2009) and a voting method. The segmentation of the atlas was used to create the mask used in the NLDR step (whole brain (union of WM, GM and CSF) or GM only).

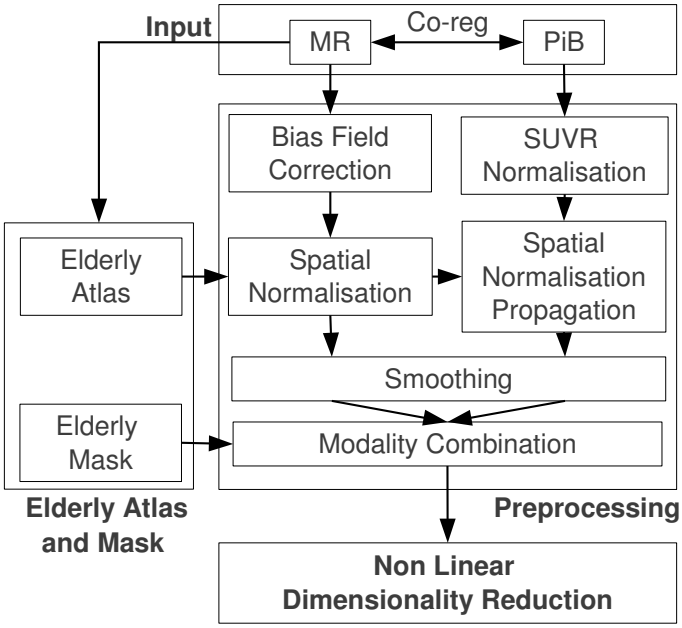


Figure 1: Overview of the algorithmic pipeline

NLDR: in this initial investigation, the NLDR was performed on the middle 2D slice using the mani Matlab implementation available at (Wittman 2005). Formally, NLDR performs the following operation : given $n$ vectors $\{x_1, \ldots, x_n\} \in \mathbb{R}^D$ and a target dimension $d < D$, $n$ corresponding vectors $\{y_1, \ldots, y_n\} \in \mathbb{R}^d$ are computed, according to some optimisation rules detailed below. In our study, the $x_i$ are the brain images (the vector coordinates are the voxel intensities), the $y_i$ are their low-dimension representations, $n$ is the number of images, $D$ is the input dimension (the number of non-zero voxels in the mask, common for all images), and $d$ is the reduced dimension. Low dimension representation of population of T1-w, PiB and combined T1-w/PiB were then studied.

Initially LLE, LEM, HEM, and LTSA were investigated for multi modality brain imaging population analysis. LEM first builds a weighted adjacency graph and then solves an eigenvalue optimisation problem based on the Laplacian operator. The weighted adjacency graph is usually a graph of k Nearest Neighbours (kNN). In this graph, each image defines one vertex, and every image is connected with an edge to its kNN. Edges are bidirectional, and weighted based on distances between images, usually using the heat kernel. ISOMAP builds a weighted neighbourhood graph (usually kNN), then computes the weights between all pairs of points using shortest paths on graphs, and finally constructs the low-dimensional embedding via an eigenvalue problem. LLE builds a kNN graph, then computes the optimal weights min-

imising the sum of the errors of linear reconstructions in the high dimensional space, and finally solve an eigenvalue problem to map to embedded coordinates. HEM identifies the kNN, obtains tangent coordinates by singular value decomposition, and then computes the embedding coordinates using the Hessian operator and eigenanalysis. LTSA uses the tangent space in the neighbourhood of a data point (typically the kNN) to represent the local geometry, and then align those tangent spaces to construct the global coordinate system for the nonlinear manifold by minimizing the alignment error for the global coordinate learning.

Although we initially investigated several algorithms, we only report the LEM results as it was the only method we found to give stable manifold structures and that did not lead to numerical issues. In particular, HEM was found to have a prohibitive processing time. On our data, LLE had numerical stability problems that resulted from nearly-singular matrices (some eigenvalues being close to zero). LTSA did not reveal any meaningful manifold structures on our data. Moreover, several target dimensions were initially investigated, however we only report the results of 2D dimensional manifolds within, as they provided more stable and meaningful structures.

As the following results were computed using LEM (Belkin and Niyogi 2003), here are additional details about this algorithm. LEM aims is a distance-based dimensionality reduction algorithm. It aims at minimizing a weighted sum of the distances in the final space (equation 1). The closer are the points in the original space, the higher are the weights.

$$\phi(Y) = \sum_{ij} w_{ij} ||y_i - y_j||^2 \qquad (1)$$

First a graph is built with edges connecting nearby points to each other. There are 2 variants: $\epsilon$-graph (nodes $i$ and $j$ are connected if $||x_i - x_j||^2 \leq \epsilon$) and $K$-NN graph (nodes $i$ and $j$ are connected if $i$ is among the $K$ nearest neighbors of $j$ or $j$ is the among $K$ nearest neighbors of $i$). In this paper, the $K$-NN version is used. The default $K$ parameter from (Wittman 2005) ($K = 8$) was used. The robustness of the manifold with regard to $K$ was also analysed. Second the edge weights are computed. Two variants are available: heat kernel ($w_{ij} = e^{\frac{-||x_i - x_j||^2}{\sigma}}$ if nodes $i$ and $j$ are connected, 0 otherwise) and simple-minded ($w_{ij} = 1$ if nodes $i$ and $j$ are connected, 0 otherwise). In this paper, we are using the simple-minded version (equivalent to a heat kernel version with $\sigma = \infty$). Third, the eigenmaps are computed. Let the the degree matrix $D$ of $W$ be the diagonal matrix with $d_{ii} = \sum_j w_{ij}$. The graph Laplacian $L$ is computed by $L = D - W$. The optimization problem can be rewritten:

$$\phi(Y) = 2Y^T LY \qquad (2)$$

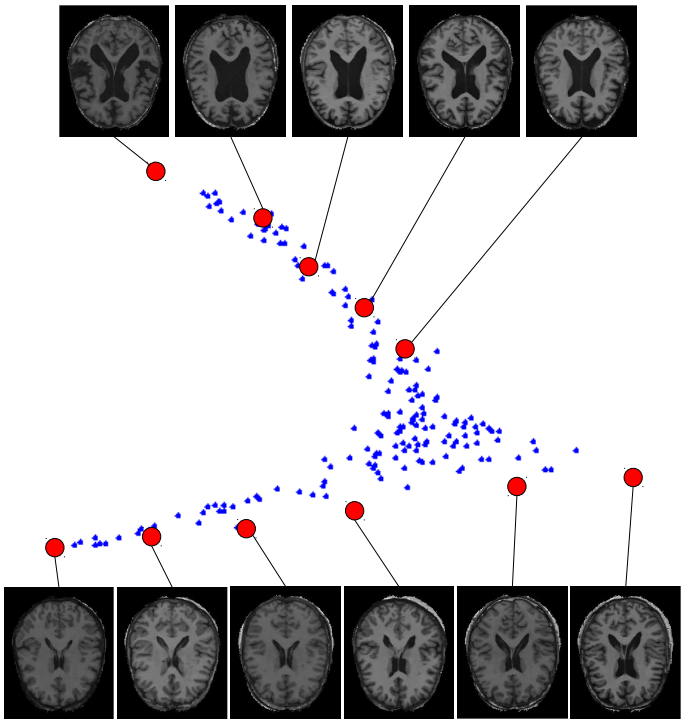

Figure 2: LEM embeddings using MR images registered with affine transformations and a global brain mask (218 images, input dimension: 23346, target dimension: 2). Several examples of corresponding images are also plotted showing increased ventricle size from bottom to top.

The low dimensional representation can therefore be found by solving the generalized eigenvalue problem:

$$Lv = \lambda Dv \qquad (3)$$

for the $d$ smallest nonzero eigenvalues. The $d$ eigenvectors $v_i$ corresponding to the smallest nonzero eigenvalues form the low-dimensional data representation $Y$.

## 3 RESULTS

The enlargement of the ventricles is one of the most obvious changes seen in MRIs of the brain as one ages. Figure 2 shows the LEM embeddings (i.e. the low dimension representation of the data) in dimension 2 with the MR images using a global tissue mask corresponding to the whole brain. A structure with two branches appears. The top branch corresponds to images with large ventricles, whereas the lower branch corresponds to smaller ventricles. Figure 3 shows that if only the central part of the brain image is used as input data (by eroding the mask), the structure of the manifold is conserved, with the same separation of ventricle sizes.

Amyloid load as observed using PET PiB is known to be related to AD. Figure 4 shows LEM embeddings in dimension 2 with PiB images. When using a global brain mask (input dimension: 23346) and im-

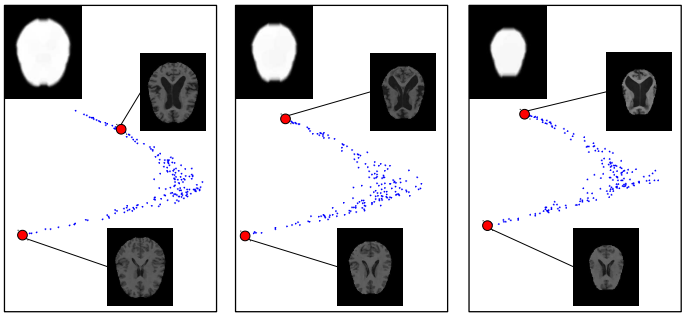

Figure 3: LEM Embeddings using MR images (registered using affine transformations) and global brain masks more and more eroded (218 images, target dimension: 2). The structure with two branches is conserved.

ages registered with affine transformations (Fig. 4a), the point cloud obtained has a similar structure as the one with MR images (Fig. 2) with two branches. The images in the bottom branch have increased PiB retention compared to the ones in the top branch. With a GM mask (input dimension: 12212) and images registered with affine transformations (Fig. 4b), the structure with two branches disappears. However, from top to bottom, the PiB retention increases. If the images are registered non-rigidly and a GM mask is used (Fig. 4c), there is a structure with 2 branches, the top branch with a low PiB retention, the other one with high PiB retention.

Figure 5a shows the LEM embeddings in dimension 2 of the data when combining the MR and PiB modalities, registered using affine transformations. Top left images have large ventricles, and bottom right images have a higher PiB retention. When images are registered non-rigidly, the structure with 2 branches appears again, and the PiB retention increases from top to bottom (Fig. 5b).

Table 1 illustrates the robustness with regard to the number of nearest neighbours K used in the neighbourhood graph. If K is too low or too high, the structure with two branches is destroyed. A value of K too high leads to jumps between different parts on the manifold.

## 4 DISCUSSION

In this paper, we investigated the use of LEM to model PET-PiB and MRI-T1-w to characterize the shape and appearance of images in a large clinical Alzheimer study. This can be particularly useful in atlas selection techniques, but can be applied in other areas. As far as shape analysis is concerned, NLDR techniques revealed that the ventricle size was the main variation in this population of brain images. The structure of the resulting 2D manifold with two branches was conserved when the cortical details were masked, leaving only the ventricles. This was expected as we used a L2 distance and many voxels were strongly affected with ventricle enlargement associated with the disease and ageing. To avoid biases from the ventricles (Fig. 4a), we examined only the GM voxels when studying PiB intensity (Fig. 4b and Fig. 4c).

Many studies advice to use an image metric based on deformations to analyse population of images (Gerber et al. 2010). Nonetheless, we have shown that a simple Euclidean distance in LEM allowed identifying a low dimensional manifold structure corresponding to some anatomical and/or intensity variations. It is expected that using L2 distance would be less computationally expensive than deformation based approaches, such as diffeomorphic or elastic registrations. This could offer faster processing especially for large databases.

## 5 ACKNOWLEDGEMENTS

Data used in this article was obtained from the AIBL study funded by the CSIRO, `www.aibl.csiro.au`.

## REFERENCES

Acosta, O., P. Bourgeat, M. A. Zuluaga, J. Fripp, O. Salvado, and S. Ourselin (2009). Automated voxel-based 3D cortical thickness measurement in a combined Lagrangian-Eulerian PDE approach using partial volume maps. *Medical Image Analysis 13*(5), 730 – 743.

Belkin, M. and P. Niyogi (2003). Laplacian eigenmaps for dimensionality reduction and data representation. *Neural Comput. 15*.

Blezek, D. J. and J. V. Miller (2007). Atlas stratification. *Medical Image Analysis 11*.

Davis, B., P. Fletcher, E. Bullitt, and S. Joshi (2007, Oct.). Population shape regression from random design data. In *ICCV*, pp. 1–7.

Ellis, K. A., A. I. Bush, D. Darby, D. De Fazio, J. Foster, P. Hudson, N. T. Lautenschlager, N. Lenzo, R. N. Martins, P. Maruff, C. Masters, A. Milner, K. Pike, C. Rowe, G. Savage, C. Szoeke, K. Taddei, V. Villemagne, M. Woodward, and D. Ames (2009). The Australian imaging, biomarkers and lifestyle (AIBL) study of aging: methodology and baseline characteristics of 1112 individuals recruited for a longitudinal study of Alzheimer's disease. *Int Psychogeriatrics 21*(4), 672–87.

Gerber, S., T. Tasdizen, P. T. Fletcher, S. Joshi, and R. Whitaker (2010). Manifold modeling for brain population analysis. *Medical Image Analysis 14*(5), 643 – 653.

Lorenzen, P., B. C. Davis, and S. Joshi (2005). Unbiased atlas formation via large deformations metric mapping. In *MICCAI 2005*.

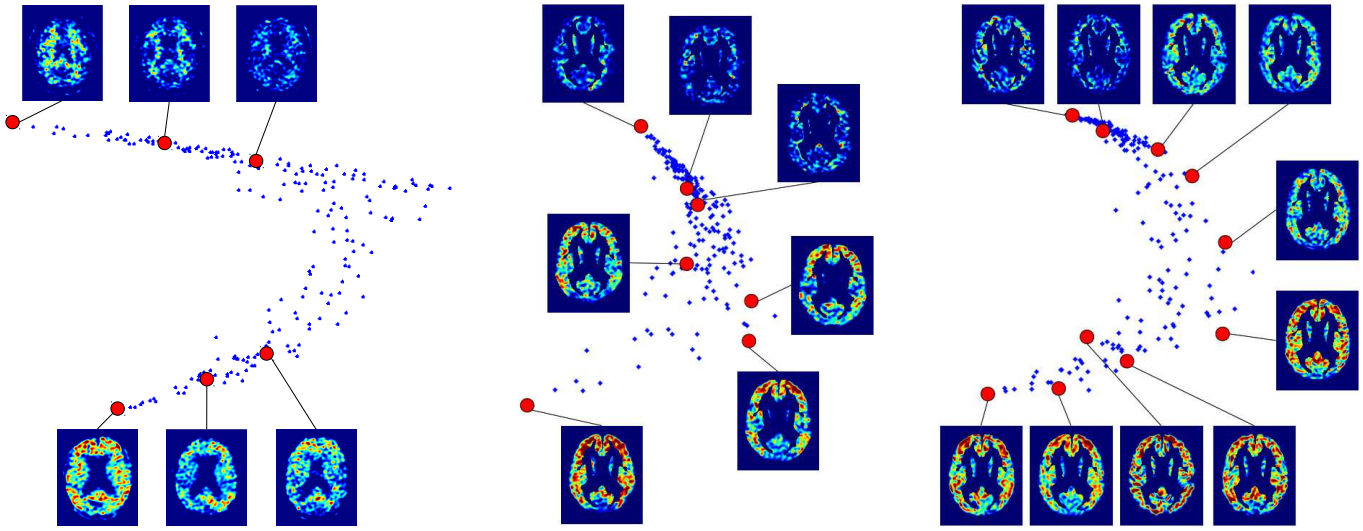

(a) Global brain mask, affine registrations (b) GM Mask, affine registrations (c) GM Mask, NRR registrations

Figure 4: LEM embeddings in dimension 2 using PiB images.

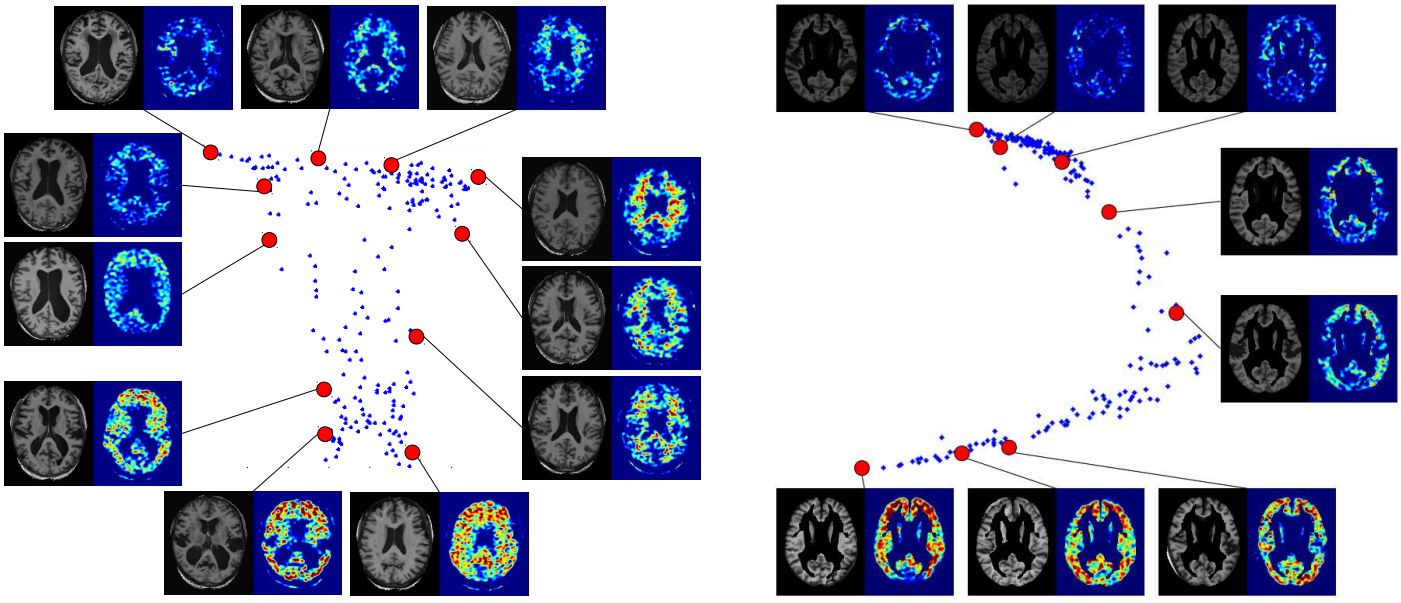

(a) With a global brain mask (input dimension: 46692) (b) With a GM mask (input dimension: 24424)

Figure 5: LEM embeddings in 2D using the combination MR + PiB (registered using affine transformations).

Table 1: Test of robustness of LEM embeddings in dimension 2 with regard to K (number of Nearest Neighbours in the graph creation), using MR images and a global brain mask. If K is too low or too high, the structure with two branches gets destroyed.

| K=2 | K=4 | K=8 |
|---|---|---|
| 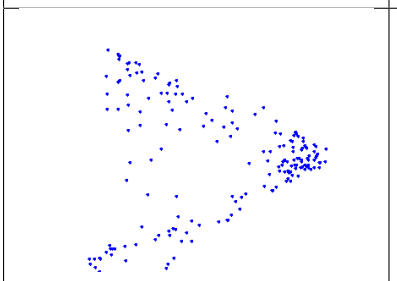 | 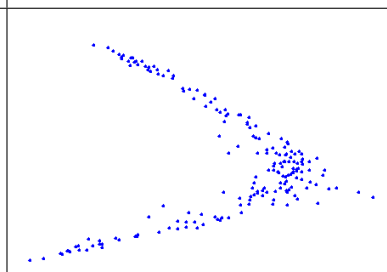 | 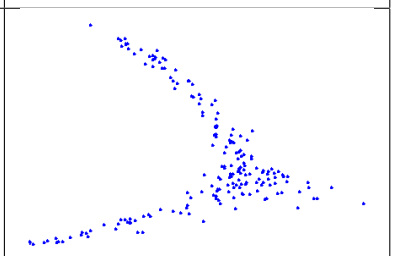 |
| **K=16** | **K=32** | **K=64** |
| 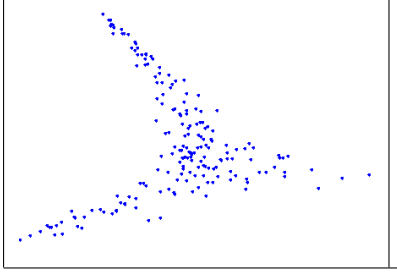 | 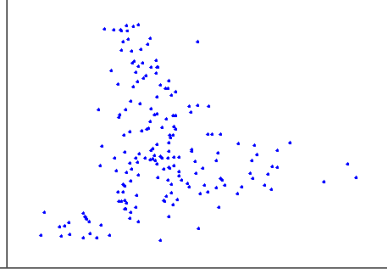 | 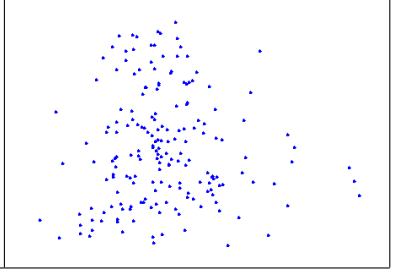 |


Raniga, P., P. Bourgeat, J. Fripp, O. Acosta, V. L. Villemagne, C. Rowe, C. L. Masters, G. Jones, G. O'Keefe, O. Salvado, and S. Ourselin (2008, Nov). Automated 11C-PiB standardized uptake value ratio. *Acad Radiol 15*(11), 1376–1389.

Sabuncu, M. R., S. K. Balci, M. E. Shenton, and P. Golland (2009, Sep). Image-driven population analysis through mixture modeling. *IEEE Trans Med Imaging 28*(9), 1473–1487.

van der Maaten, L., E. Postma, and H. van den Herik (2007). Dimensionality reduction: A comparative review. *10*(February), 1–35.

Wittman, T. (2005). MANIfold learning matlab demo. `http://www.math.ucla.edu/~wittman/mani`. Version 2.5.

Wolz, R., P. Aljabar, J. V. Hajnal, A. Hammers, D. Rueckert, and the Alzheimer's Disease Neuroimaging Initiative (2009). LEAP: learning embeddings for atlas propagation. *NeuroImage*.